

Star-Forming AGN Host Galaxies

Peter Barthel

*Kapteyn Astronomical Institute, P.O. Box 800, 9700 AV Groningen,
The Netherlands*

Abstract

The symbiosis of nuclear activity and star-formation in galaxies, as manifested in their spectral energy distributions (SEDs) is reviewed. Attention is drawn to an Hertzsprung-Russell diagram-equivalent for such objects, as well as to the importance of the SEDs in cosmological context.

Key words: galaxies: active, galaxies: starburst, quasars: infrared

1 Introduction

Let me start this review (the first paper at this workshop) by showing you a picture of good-old IRAS. It is fair to say that IRAS added a new dimension to the parameter space of galaxies: dust emission. This dimension is the very reason for our get-together! Not only has the highly diverse dust content of normal and active galaxies become apparent, but a new class of very dusty galaxies has also emerged: the UltraLuminous Infrared Galaxies (ULIRGs). This review will primarily discuss the active galaxies among the former group, but also deal with the latter group, in their relation to the former.

A key issue in contemporary astrophysics is the cosmologically evolving star-formation activity. Nuclear activity, taken here to mean accretion driven energy generation, and circumnuclear star-formation activity in galaxies, are sometimes seen to go hand in hand (e.g., NGC 1068: Schinnerer et al. 2000; Mkn 231: Taylor et al. 1999). The question arises whether the resemblance of the cosmic star-formation history diagram (Madau et al. 1996) and the plot of evolving QSO space density (in particular the $z \approx 2.5$ peak; e.g., Shaver et al. 1996) is purely coincidental. In this review I wish to convey the message that AGN host galaxies offer excellent opportunities to study the history

Email address: pdb@astro.rug.nl (Peter Barthel).

of star-formation over a substantial cosmic time span, and I will describe the usefulness and the unique character of the global Spectral Energy Distribution (SED) of these objects in such studies. Indeed, as judged from these SEDs, a substantial fraction of (nearby) QSO host galaxies display vigorous star-formation. I will draw attention to a far-infrared AGN Hertzsprung-Russell diagram that may prove useful in the study of the interconnection between active galaxies and ULIRGs.

2 Dust in normal and active galaxies

The FIR SED of a normal galaxy is commonly believed to consist of a cold ($T \sim 15$ K) component and a warmer ($T \sim 20$ – 60 K) component (e.g., Helou 2000). The former is the well known large scale cirrus component, being energized by the diffuse interstellar radiation field of the, primarily, old stellar population. The latter originates from dust in star-forming regions, i.e., regions containing massive young stars which provide a strong, dust-heating UV photon field (and moreover, yield supernovae). Depending on the relative strength of these two components a galaxy will display a cold, intermediate temperature, or warm FIR SED. While passively evolving spirals have a steeply rising SED from $60 \mu\text{m}$ to $100 \mu\text{m}$, with¹ average $\alpha_{60}^{100} \sim -1.5$ (or equivalently $\log S(60)/S(100) \sim -0.3$) and average $\alpha_{25}^{60} \sim -2.5$, starburst galaxies such as M82 and Arp 220 are warmer, having $\alpha_{60}^{100} \sim 0$ (and α_{25}^{60} in the range -2 to -3). The strength of the warm dust component is correlated with the optically thin synchrotron radio emission – this is the well known radio-FIR correlation (e.g., Condon 1992).

Active galaxies display still warmer dust, drawing additional heating input from the hard continuum radiation of the active nucleus. Seyfert galaxies for instance display warm FIR SEDs, and the FIR warmth as quantified by the α_{25}^{60} index indeed appears to be a useful AGN selection criterion: De Grijp et al. (1985) found a high fraction of Seyferts among galaxies having α_{25}^{60} flatter than -1.5 . Early on in the IRAS survey the nearby broad-line radio galaxy 3C 390.3 was suspected to have even warmer dust: Miley et al. (1984) reported a pronounced $25 \mu\text{m}$ peak in this object. Van Bemmelen (these Proceedings) deals with the far-infrared SEDs of the BLRG class, suggesting that in fact there is not an excess of hot dust but a deficit of cool dust in these $25 \mu\text{m}$ peakers.

While ground-breaking work on FIR SEDs in galaxies was carried out by IRAS, ISO has put this research on a more quantitative basis. For instance, Rodríguez Espinosa et al. (1996) and Pérez García et al. (1998) used ISO

¹ $S_\nu \propto \nu^\alpha$ adopted

data to further constrain the multi-temperature dust model for Seyfert galaxies. From detailed measurements of the FIR SEDs they infer the presence of warm dust ($T \sim 150$ K), presumably heated by AGN, and cooler dust ($T \sim 45$ K), presumably heated by young stars. Also, the cold cirrus component could be identified in a number of cases. Subsequent optical imaging (Rodríguez Espinosa & Pérez García 1997) demonstrated that indeed, the warm and cool dust are respectively AGN and host galaxy related. Bimodal dust temperature distributions were also measured in the interacting Antennae galaxies NGC 4038, 39 and the ultraluminous infrared galaxies NGC 6240 and Arp 220 (Klaas et al. 1997). In these objects the warm dust is believed to be powered by starburst activity, the relative strength of the warm component w.r.t. the cool component being governed by extinction within the system.

While the star-formation related dust cannot be easily linked to the color and luminosity of the host galaxy (e.g., Helou 2000), such an astrophysical connection must be present. Bregman et al. (1998) for instance found that FIR-bright early type galaxies are more luminous in $H\alpha$, $H I$ and CO lines as compared to their normal counterparts. In the same vein, Clements (2000) showed that among radio-quiet QSOs the ones having cool colors (hence substantial cool dust besides the AGN related hot dust) stood out with a higher FIR luminosity and higher incidence of distorted optical host morphology. The latter is generally taken to imply enhanced star-formation (e.g., Mazzarella et al. 1991).

3 Dust in quasars and radio galaxies

As for the more powerful AGN in the distant universe, it should be first noted that IRAS detected primarily radio-loud objects, with a dominant contribution from flat (radio-)spectrum objects. This calls for a careful examination of the SEDs of radio-loud quasars and radio galaxies, taking their detailed radio characteristics into account. The optical–FIR–radio SED of the well known radio galaxy Cygnus A (3C 405), as compiled by Ilse van Bemmelen, is shown in Fig. 1, together with a model fit of optically thin black bodies. The infrared spectral indices of Cyg A are: $\alpha_{60}^{100} = +1.1$ and $\alpha_{25}^{60} = -1.3$.

Consistent with the FIR SEDs of normal and Seyfert galaxies, we see cold, cool and warm dust in Cyg A. The pronounced cool ($T = 55$ K) dust luminosity suggests a substantial level of star-formation in the Cyg A host galaxy. The fact that the ratio of FIR and radio luminosity for Cyg A is substantially different from the general radio galaxy population is nevertheless attributed to the anomalously high radio luminosity of the object (Barthel & Arnaud 1996). As can be readily seen, non-thermal FIR radiation, i.e., the short wavelength tail of the nuclear continuum, has an almost negligible strength. Combining

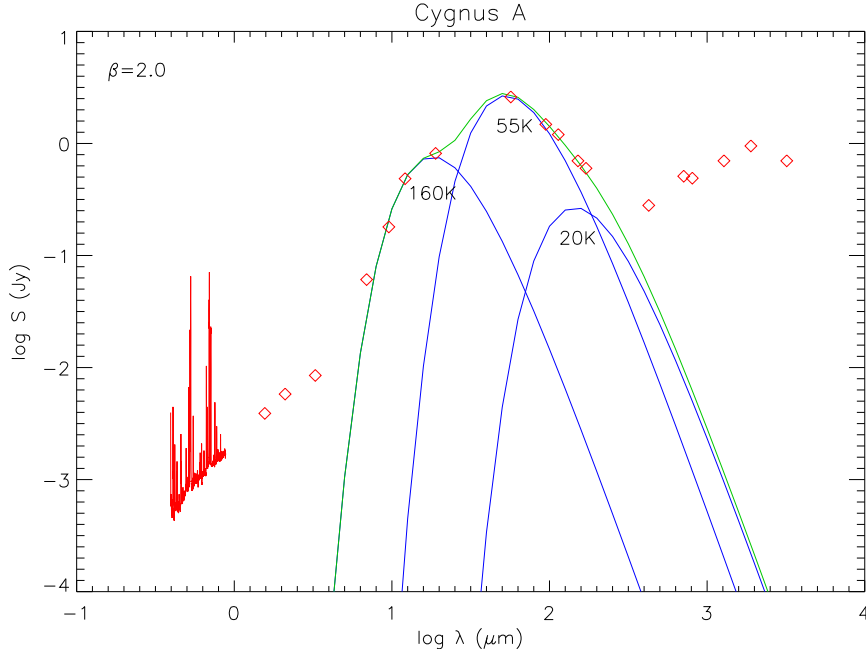


Fig. 1. The optical–NIR–FIR–submm–radio SED for Cygnus A. Ground-based optical, near-IR and radio data are combined with ISO photometry. The sub-mm, mm, and cm points reflect the core emission, obviously excluding the extended radio lobes.

clear detections at about ten wavelengths, no other radio galaxy or quasar has its infrared SED so well determined.

As for the quasars measured by IRAS, very few distant radio-quiet QSOs and only a handful of steep-spectrum 3CR QSRs were detected (Neugebauer et al. 1986). Early on, QSR 3C 48 was recognized as an extraordinary luminous FIR emitter (Neugebauer et al. 1985). QSR 3C 446 was also found to be infrared luminous, but as nicely illustrated by its IRAS measured variability (Neugebauer et al. 1986), nonthermal radiation must be dominating the 3C 446 SED, in line with its identification as a Blazar. Blazars were soon recognized as a class of their own, with smooth albeit variable radio–FIR–optical continua (Edelson & Malkan 1987, Impey & Neugebauer 1988, Brown et al. 1989). The IRAS radio galaxy study by Golombek et al. (1988) yielded a couple dozen detections but only two objects beyond $z = 0.2$. However, despite the limitations of these data, some interesting trends emerged for various classes of powerful AGN. For instance, Golombek et al. found that the radio galaxy FIR strength reflected their emission line strength. Heckman et al. (1992, 1994), employing improved IRAS data analysis routines, compiled infrared SEDs for ensembles of AGN. They reported that FR1 (edge-darkened) radio sources were about a factor of four less luminous in the FIR as compared to FR2 (edge-brightened, hotspot) sources, and they confirmed the presence of a hot $25\mu\text{m}$ dust component in the class of broad-line radio galaxies. They also reported subtle differences in FIR output between FR2 radio galaxies and QSRs, discordant with predictions of the simple orientation-based unification model.

The work of Hes et al. (1995) increased the detection rate of distant 3C objects and provided a clear picture of the mechanisms involved. They confirmed the Heckman et al. finding that quasars are somewhat brighter in the far-infrared than radio galaxies, but pointed out that beamed non-thermal radiation might be (at least in part) responsible for this difference. The $60\mu\text{m}$ strength being correlated with the radio core strength, it is unlikely that the Rowan-Robinson (1995) two-component dust model applies to radio-loud objects: the AGN strength is probably also reflected in the long wavelength FIR emission. Hoekstra et al. (1997) modeled FIR beaming, and quantified its effect on the FIR SED, as a function of radio beaming. Hes et al. (1995) also discovered that the probability of detecting a radio galaxy in the far-infrared is enhanced by optical N-type morphology, in connection with either broad lines or the combination of compact radio structure and blue optical colors. The latter fact was clearly underlined by Willott et al. (2000), who discovered that the redshift of the IRAS detected compact radio galaxy 3C 318 is 1.5 rather than 0.7: 3C 318 is the most distant 3C source detected by IRAS, harbouring a dust luminosity of approximately $10^{14} L_{\odot}$. The high FIR luminosity of the QSR 3C 48 could be understood along similar lines. The subgalactic size radio source is hosted by a galaxy merger displaying luminous young star clusters and HII regions (Kirhakos et al. 1999, Canalizo & Stockton 2000b) as well as bright molecular gas emission (Wink et al. 1997). The FIR luminosity of 3C 48 must be connected to ongoing star-formation.

Combining IRAS with cm and mm data, Van Bemmelen et al. (1998) further quantified the level of FIR beaming in double-lobed quasars: they found its magnitude to be modest, and not sufficient to explain the difference with radio galaxies. Using the PHOT instrument on board ISO Haas et al. (1998) confirmed and refined the picture as drawn by IRAS. In particular, the contributions of beamed non-thermal and presumed aspect-independent thermal FIR emission could be isolated in the SED of blazar 3C 279, and the multi-component nature of its dust emission became apparent. It will by now be clear why I started my examination of the AGN FIR SED components with the radio-loud subclass: these offer the advantage that their jet orientation w.r.t. the observer is known so that orientation dependence can be taken into account. Focussing on the unification issue, such was again done by Van Bemmelen et al. (2000), examining ISO photometry of samples of quasars and radio galaxies. Apparent disagreement with predictions of the unification scheme may be attributed to small anisotropy effects (but see also Müller et al. in these Proceedings).

Polletta et al. (2000) examined ISOPHOT measurements of the FIR SEDs of quasars, dealing with various classes of radio-loud and radio-quiet objects. They present average quasar SEDs and conclude that AGN powered far-infrared emission dominates the SED, but that it is supplemented by star-burst powered FIR emission. The latter is observed in radio-loud and radio-

quiet QSOs, at comparable strength in both classes. Haas et al. (2000; see also Haas' contribution in these Proceedings) describe ISO measurements of the FIR SEDs of PG QSOs. The SEDs suggest strong dust emission, drawing power from both the AGN and starburst activity.

While in the case of radio-loud quasars and radio galaxies radio images at arcsecond and milliarcsecond resolution irrefutably demonstrate that the activity originates in a subparsec sized volume, such is not readily apparent in radio-quiet objects. Given the fact that radio-quiet QSOs appear to follow the radio-FIR correlation for star-forming systems (which include 30 Doradus, irregular galaxies, spiral galaxies and ultraluminous infrared galaxies) it has been proposed that QSOs may be powered by starburst activity as well (e.g., Sopp & Alexander 1991). Analyses by Rush et al. (1996) and Giuricin et al. (1996) have in the meantime shown that excess radio emission is present in Seyfert galaxies, calling for a non-thermal AGN. The issue for the more distant and powerful QSOs remains controversial. I will return to this issue later.

In summary, the FIR SEDs of active galaxies are composed of cold ISM dust emission, cool star-formation dust, warm AGN heated dust and possibly a beamed nonthermal component. Describing the FIR SEDs in terms of discrete temperature components (besides the smooth synchrotron continuum) is obviously a naive simplification, but so far seems to work reasonably well.

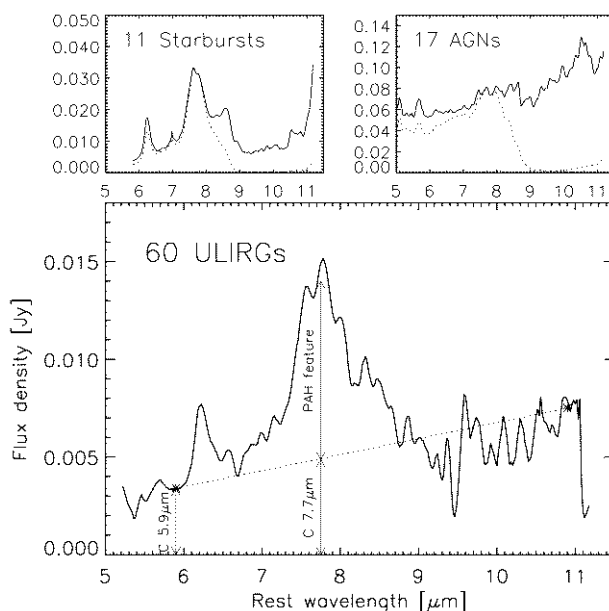


Fig. 2. The relative strength of the 7.7μm PAH feature for the average (nearby) AGN, starburst and ultraluminous infrared galaxy, from Lutz et al. (1998).

4 Dust and gas in ULIRGs and QSOs

We have seen in the previous sections that both AGN heated and star-formation heated dust can be recognized in AGN FIR SEDs. Prime examples of systems undergoing vigorous star-formation are the ULIRGs (e.g., Sanders & Mirabel 1996). Also given the fact that radio-quiet QSOs and ULIRGs obey the same radio-FIR correlation (see for instance Figures 3 and 4 in Colina & Pérez-Olea 1995), the question as to the interconnection between AGN and starbursting ULIRGs is a long standing one – e.g., Sanders et al. (1988). At least for nearby objects, ISO spectroscopy has indicated that the ionization stages of AGN and ULIRGs are different: high ionization lines ([O IV], [Ne V]) appear in the mid-infrared spectra of the former but not the latter class (Lutz et al. 1996, Lutz et al. 1999). Also the relative strength of the PAH features appears to be a useful diagnostic – see Fig. 2, taken from Lutz et al. (1998), which shows this PAH/continuum ratio for the average AGN, starburst galaxy and ULIRG. Spoon et al. (2000) has recently pointed out a caveat when using this diagnostic, and it should also be noted that these diagnostics have not yet been applied to luminous QSOs.

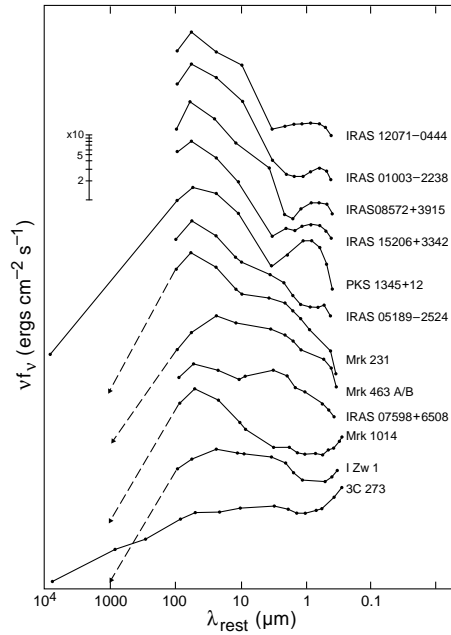


Fig. 3. Radio-FIR-optical SEDs for warm IRAS sources (Sanders et al. 1988)

Section 2 already addressed the relative strength of warm and cool dust, and specifically the FIR SED spectral slope α_{25}^{60} , to isolate AGN among star-forming galaxies. The usefulness of this index is nicely illustrated by Fig. 3, a compilation of SEDs of relatively warm ultraluminous infrared sources, taken from Sanders et al. (1988): a range of spectral slopes is seen, from fairly steep

to flat/inverted. Fig. 4 combines α_{25}^{60} with α_{60}^{100} data, for IRAS detected QSOs and ULIRGs. QSOs cluster in the area $\alpha_{25}^{60} \approx \alpha_{60}^{100} \approx -1$. Well-known star-forming QSOs (e.g., Canalizo & Stockton 2000a) occupy the area close to the ULIRGs in this FIR color-color diagram. Indeed α_{25}^{60} appears a good discriminator: in fact some strongly star-forming QSOs (genuine PG QSOs!) are too ‘cool’ to classify as AGN under the De Grijp et al. (1985) $\alpha_{25}^{60} > -1.5$ criterion. Such ‘cool’ QSOs were addressed by Clements (2000 – see Section 2) and are also under study by Stockton and collaborators, Sanders and collaborators, and by our group – the next section describes this work.

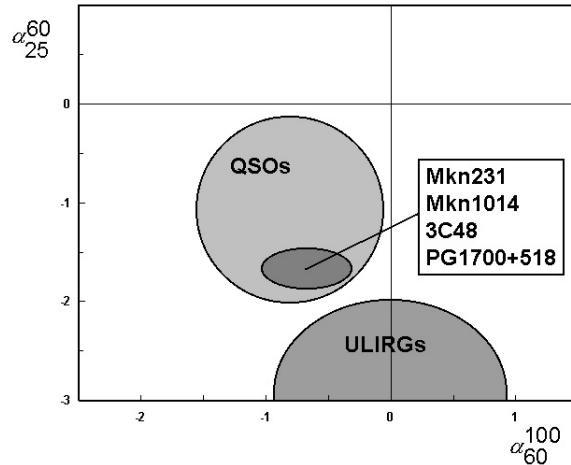


Fig. 4. IRAS color-color diagram for quasars and ULIRGs

5 The starburst–AGN symbiosis: source evolution?

As we have seen in the previous section, the far-infrared spectral index α_{25}^{60} broadly speaking allows to address the relative importance of AGN-activity and starburst-activity in – at least not too distant – galaxies. Attempts have also been made to combine an infrared spectral index with the relative PAH strength (e.g., Lutz et al. 1998) and with line ratio’s (e.g., Kewley et al. 2001) in such assessments. A Groningen-lead study (in a collaborative effort with researchers in Hawaii, Socorro, Cambridge (UK) and Hertfordshire) has shown that the FIR SEDs indeed present a powerful tool, particularly 25 and 60 μm photometry in combination with sensitive high-resolution radio imaging.

Our group has obtained and analysed deep radio (VLA), optical/nearIR (ESO; La Palma, including Carlsberg Meridian Circle astrometry), as well as improved IRAS data for a sample of 16 Seyfert galaxies having $z < 0.02$, and 27 radio-quiet PG QSOs having $0.02 < z < 0.4$. These complementary sets of active galaxies span a wide range (3.5 orders of magnitude) of luminosities. These are expressed as $L(12\mu\text{m})$, and hence predominantly reflect the AGN strength

(e.g., Spinoglio & Malkan 1989). The radio-imaging, reaching noise levels of $\sim 30 \mu\text{Jy}$, combined with the optical astrometry yields AGN positions to a 3σ accuracy of $\sim 0.4 \text{ arcsec}$. This allows assessment of the star-formation driven radio emission. The radio data of these – I stress – radio-quiet active galaxies are being combined with far-infrared photometry, yielding u -parameters $\log S_{60\mu}/S_{6\text{cm}}$ (see e.g., Condon & Broderick 1988), which permit the determination of the relative contributions of nuclear activity and star-formation. Most Seyfert galaxies have infrared detections (at 25 and $60 \mu\text{m}$), in contrast to about half of the PG QSOs. Also the ratios of the $60 \mu\text{m}$ and blue flux densities were compiled.

Figure 5 shows α_{25}^{60} as function of the u -parameter. Normal star-forming spirals, obeying the radio-FIR correlation, have u values in the range 2.4–3.0. It is seen that the more powerful (radio-quiet but *not* radio-silent) QSOs have flatter indices than the Seyferts, and that excess nuclear radio emission (i.e., $u < 2.4$) leads to warmer dust for both classes.

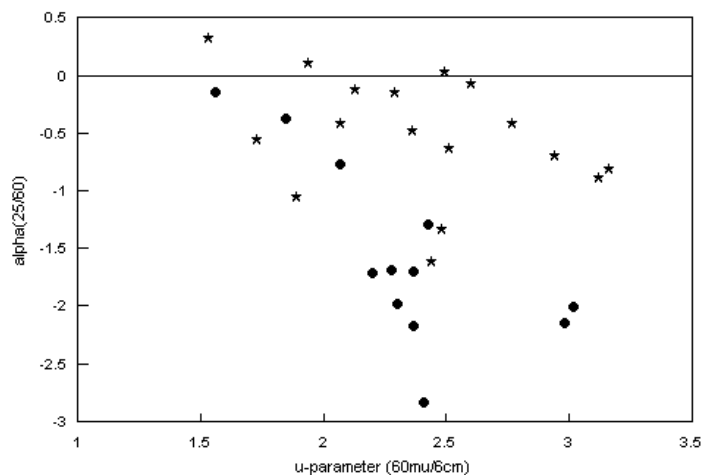


Fig. 5. Infrared spectral index α_{25}^{60} as function of u -parameter $\log S_{60\mu}/S_{6\text{cm}}$

In order to quantify the heating effect of the AGN luminosity, I plot in Figure 6 the FIR spectral index as function of the $12 \mu\text{m}$ luminosity. The trend of warmer dust with increasing AGN luminosity is clearly seen. Examination of the u -parameters results in the distributions as marked with light and dark shading. Light shading indicates objects having $u < 2.5$, having excess nuclear radio emission. Their $60\mu/B$ ratios are low. Dark shading indicates objects with merely diffuse radio emission, $u \sim 2.7$ and $60\mu/B$ ratios typically a factor 5 – 10 higher. Note that particularly for the QSOs the B -band magnitude measures the AGN strength.

On the basis of these measurements I conclude that star-formation plays a stronger role in the lower half of the diagonal strip than it does in the upper half. Could this be an evolutionary effect, during the lifetime of the

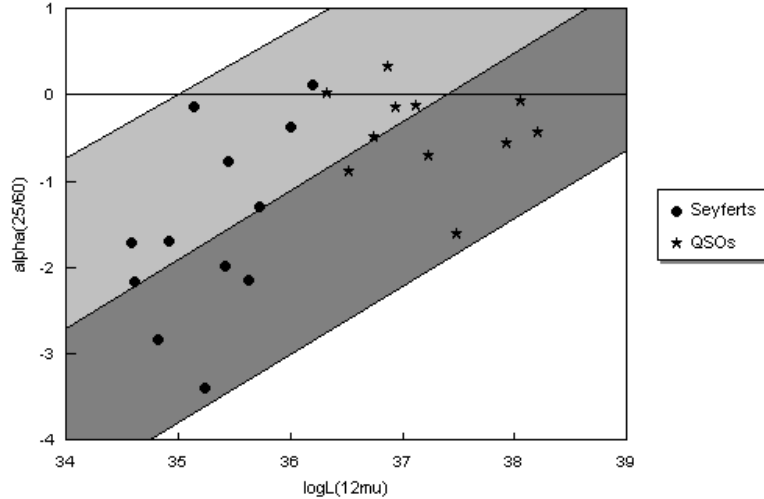


Fig. 6. Infrared spectral index α_{25}^{60} as function of AGN luminosity, with star-formation being relatively important (dark grey) and unimportant (light grey).

active galaxy? Figure 7 is the same plot as Figure 6, but with the well-known (U)LIRGs Arp 220, NGC 6240, Mkn 231 and star-forming Seyfert galaxies NGC 1808, NGC 7469, NGC 7552 added. These strongly star-forming systems indeed appear in and below the lower part of the diagonal strip, in line with the picture where the AGN phase is preceded by a gradually weakening starburst phase. Note that for the six star-formers (open symbols) the $12\mu\text{m}$ luminosity is probably not the optimal indicator of their FIR luminosity. Their actual luminosity points may lie more to the right. When rotated by 90° , figure 7 displays luminosity vs. temperature, and can thus be considered as the active galaxy equivalent of the classical Hertzsprung-Russell diagram. Larger samples and detailed analysis of the star-formation histories (e.g., Canalizo & Stockton 2000a, Canalizo 2000) may permit to draw evolutionary tracks. JCMT observations of the molecular gas in QSO hosts are currently being analyzed by our group to test the evolutionary scenario. Given that roughly half of the AGN occupy the strip where star-formation is important, the similarity of the cosmic star-formation history and the quasar space density history referred to in the introductory section may indeed *not* be coincidental.

6 Summary

The $60\mu\text{m}$ luminosity, when normalized with the $25\mu\text{m}$ (or the $12\mu\text{m}$), the blue or the radio luminosity, permits one to assess the absolute and relative strength of star-formation and nuclear activity in active galaxies and quasars. The FIR temperature can be combined with measures of the bolometric luminosity to yield an intriguing AGN Hertzsprung-Russell diagram, which among other things suggests that star-formation plays an important role. These photometric ratios can be obtained in a straightforward manner for the faint dis-

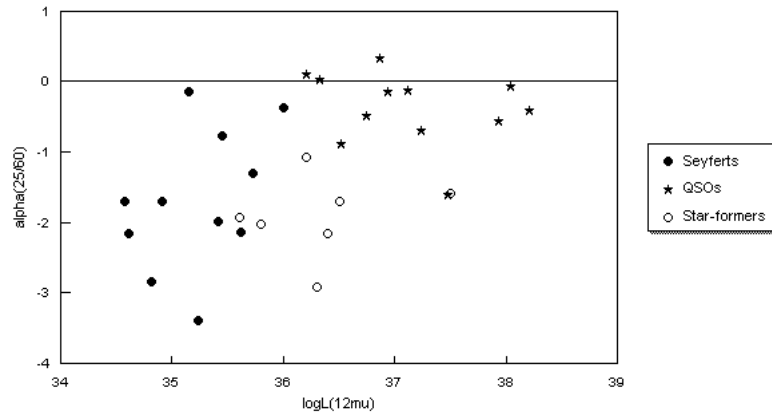


Fig. 7. An AGN Hertzsprung-Russell diagram?

tant objects to be measured in large quantities with upcoming space-infrared missions, such as SIRTf, ASTRO-F and FIRST/Herschel.

7 Acknowledgements

Thanks are due to Dieter Lutz, David Sanders and Ilse van Bemmell, who allowed me to reproduce figures, and to Jim Higdon who read the manuscript. I acknowledge a long collaborative effort with Bob Argyle, Jeroen Gerritsen, Magiel Janson, Johan Knapen, David Sanders and Dick Sramek.

References

- Barthel P.D., Arnaud K., 1996, M.N.R.A.S. 283, L45
- Bregman J.N., Snider B.A., Grego L., Cox C.V., 1998, ApJ 499, 670
- Brown L.M.J., Robson E.I., Gear W.K., et al., 1989, ApJ 340, 129
- Canalizo G., 2000, PhD Thesis (University of Hawaii)
- Canalizo G., Stockton A., 2000a, AJ 120, 1750
- Canalizo G., Stockton A., 2000b, ApJ 528, 201
- Clements D.L., 2000, M.N.R.A.S. 311, 833
- Colina L., Pérez-Olea D.E., 1995, M.N.R.A.S. 277, 845
- Condon J.J., 1992, ARAA 30, 575
- Condon J.J., Broderick J.J., 1988, AJ 96, 30
- De Grijp M.H.K., Miley G.K., Lub J., De Jong T., 1985, Nature 314, 240
- Edelson R. A., Malkan, M. A., 1987, ApJ 323, 516
- Giuricin G., Fadda D. Mezzeti M., 1996, ApJ 468, 475
- Golombek D., Miley G.K., Neugebauer G., 1988, AJ 95, 26
- Haas M., Chini R., Meisenheimer K., et al., 1998, ApJ 503, L109

Haas M., Müller S.A.H., Chini R., et al., 2000, A&A 354, 453
 Helou G., in *Infrared Astronomy: Today and Tomorrow*, Les Houches Summer School (eds. F. Casoli and J. Lequeux), 2000, astro-ph/0005198
 Heckman T.M., Chambers K.C., Postman M., 1992, ApJ 391, 39
 Heckman T.M., O’Dea C.P., Baum S.A., Laurikainen E., 1994, ApJ 428, 65
 Hes R., Barthel P.D., Hoekstra H., 1995, A&A 303, 8
 Hoekstra H., Barthel P.D., Hes R., 1997, A&A 319, 757
 Impey C.D., Neugebauer G., 1988, AJ 95, 307
 Kewley L.J., Heisler C.A., Dopita M.A., Lumsden, S., 2001, ApJS 132, 37
 Kirhakos S., Bahcall J.N., Schneider D.P., Kristian J., 1999, ApJ 520, 67
 Klaas U., Haas M., Heinrichsen I., Schulz B., 1997, A&A 325, L21
 Lutz D., Genzel R., Sternberg A., et al. 1996, A&A 315, L137
 Lutz D., Spoon H.W.W., Rigopoulou D., Moorwood A.F.M., Genzel R., 1998, ApJ 505, L103
 Lutz D., Veilleux S., Genzel R., 1999, ApJ 517, L13
 Madau P., Ferguson H.C., Dickinson M.E., et al., 1996, MNRAS 283, 1388
 Mazzarella J.M., Bothun G.D., Boroson T.A. 1991, AJ 101, 2034
 Miley G., Neugebauer G., Clegg P.E., et al. 1984, ApJ 278, L79
 Neugebauer G., Soifer B.T., Miley G.K., 1985, ApJ 295, L27
 Neugebauer G., Miley G.K., Soifer B.T., Clegg P.E., 1986, ApJ 308, 815
 Pérez García A.M., Rodríguez Espinosa J.M., Santolaya Rey A.E., 1998, ApJ 500, 685
 Polletta M., Courvoisier T.J.-L., Hooper E.J., Wilkes B.J., 2000, A&A 362, 75
 Rodríguez Espinosa J.M., Pérez García A.M., Lemke D., Meisenheimer K., 1996, A&A 315, L129
 Rodríguez Espinosa J.M. & Pérez García A.M., 1997, ApJ 487, L33
 Rowan-Robinson M., 1995, M.N.R.A.S. 272, 737
 Rush B., Malkan M.A., Edelson R.A., 1996, ApJ 473, 130
 Sanders D.B. & Mirabel I.F., 1996, ARAA 34, 749
 Sanders D.B., Soifer B.T., Elias J.H., Neugebauer G., Matthews K., 1988, ApJ 328, L35
 Schinnerer E., Eckart A., Tacconi L. J., Genzel R., Downes D., 2000, ApJ 533, 850
 Shaver P.A., Wall J.V., Kellermann K.I., Jackson C.A., Hawkins M.R.S., 1996, Nature 384, 439
 Sopp H.M. & Alexander P., 1991, M.N.R.A.S. 251, 14P
 Spinoglio L. & Malkan M.A., 1989, ApJ 342, 83
 Spoon H.W.W., Keane J.V., Tielens A.G.G.M., Luz D., Moorwood A.F.M., 2000, A&A 365, L353
 Taylor G.B., Silver C.S., Ulvestad J.S., Carilli, C.L., 1999, ApJ 519, 185
 Van Bemmell I.M., Barthel P.D., Yun, M.S., 1998, A&A 334, 799
 Van Bemmell I.M., Barthel P.D., de Graauw M.W.M., 2000, A&A 359, 523
 Willott C.J., Rawlings S., Jarvis M.J., 2000, M.N.R.A.S. 313, 237
 Wink J.E., Guilloteau S., Wilson T.L., 1997, A&A 322, 427